



## Petrology and Geochemistry of Gole Pillow Basalt in Penjween area

### Kurdistan Region- NE Iraq

Jabbar M. A. Qaradaghi , Yousif O. Mohammed , Salim A. Aziz.

Department of Geology, College of Science, University of Sulaimani, Sulaymaniyah, Iraq.

<https://doi.org/10.25130/tjps.v24i7.460>

#### ARTICLE INFO.

##### Article history:

-Received: 15 / 10 / 2019

-Accepted: 12 / 11 / 2019

-Available online: / / 2019

**Keywords:** Gole. Pillow Basalt. Alkaline Basalt. OIB. Penjween. Kurdistan Region.

##### Corresponding Author:

##### Name:

Jabbar M. A. Qaradaghi

##### E-mail:

[jabbar.faraj@univsul.edu.iq](mailto:jabbar.faraj@univsul.edu.iq)

##### Tel:

#### ABSTRACT

The petrological, morphometric and geochemical analyses of pillow lava from Gole village (Penjween town) Sulaimani city Northeastern Iraq have been undertaken. The Gole Pillow basalt (GPB) extruded, in the form of pillow and sheet flow into the Qulqula radiolarite Formation. The basaltic intrusion restricted to a small area of about 100 m<sup>2</sup> within Penjween-Walash zone in the Zagros Suture Zone (ZSZ) of Iraq. The investigated area divided into two sections GPB1 and GPB2. It is envisaged that the studied area distinct two episodes of submarine alkaline eruptions that produced pillowed lavas that differently interacted with seawater to produce different morphologies and geochemistries. The pillows of the GPB1 section well exposed all along the Shalair river near Gole village. Although the pillows of the GPB2 section altered due to low-grade metamorphism and late hydrothermal processes, their igneous textures are still preserved. GPB samples are mostly phyrlic in nature and show porphyritic or sub-ophitic textures.

Petrographically, most of the GPB rock samples appeared as amygdaloidal and vesicular aphanitic basalt. Large phenocryst of hypersthene with schiller structure is present within a matrix of longer quenched plagioclase. Numerous small euhedral grains of opaque minerals like ilmenite and hematite are dispersed in the fine groundmass.

Morphological features show that the GPB appeared as spheroidal and lobate to tubular individual pillows. Although some pillow extends 2 meters with a foreset distribution some others show cracked with irregularly jointed surface and larger vesicles partly filled with calcite and quartz.

Geochemical investigation of GPB exhibit high TiO<sub>2</sub> (3.42 – 3.84 wt.%), Fe<sub>2</sub>O<sub>3</sub> (14.84–19.93 wt.%), and high Zr/Nb and Zr/Y ratios respectively (5.85 – 7.2) (7.10-11.40). The content of alkalis, with the Nb/Y ratio ≥ 1.4, and silica, as well as many trace element discrimination diagrams, classify the GPB as alkaline basalts.

The field, stratigraphic relationships, and geochemistry of the GPB and associated clastic and carbonate sediments suggest that the pillow lavas were emplaced in a shallow marine marginal within plate basin. The overall geochemistry of GPB resembles that of alkaline basalts generated in within-plate ocean island settings (OIB-type).

#### 1. Introduction

Generally, various forms of lava will produce when hot lava flows enter standing water, they appear either as tongues or more equidimensional blob-like structures, all are called pillows [1]. Pillows form as hot lava is extruded from an active vent and forms a chilled visco-elastic margin on contact with cold ocean water. This crust would be puffed by volatiles

and a continued flux of lava from the vent to the flow front via feeder channels, forming the typical lobate pillow structure [2]. Developed pillows grow as parent pillows stretch and form cracks that extrude fresh lava [3]. General categories of morphology determined from subaerial and submarine observation of lava are pillowed, lobate and sheet flows [4].

Pillow lavas in Kurdistan region have been studied earlier by several authors including [5]; [6]; [7]; [8]; [9]; [10] and [11]. Although all studied areas are located along the Zagros Suture Zone (ZSZ), there is no such a report (document) among previous literature on pillow lavas along Main Zagros Reverse Fault (MZRF). Alkaline rocks in the Zagros are represented mainly by basalts which displaying a clear alkaline nature [12]. Their study concluded from the discrimination diagram that these volcanic units from the MZTZ ophiolites show a continuous compositional variation from the less enriched to the more enriched rocks and their overall geochemistry resembles that of alkaline basalts generated in within-plate ocean island settings (OIB-type).

The Pillow Basalts of Penjween area (GPB) were nominated based on the locality names as the Gole Pillow Basalt (nearest village name). However, detailed geological and precise investigations are still rare in the Penjween area and this might be due to topography and the presence of landmines of the area. Petrologic and geochemical classifications of the area were made based on analyses of samples collected from two sections of the studied area.

This study presents a higher-resolution investigation of two sections through some pillow lavas at Gole area than previous works (Fig. 1). The main objective of this study is to identify and document the petrology and morphology of the GPB from the Penjween area, Kurdistan Region, Northeast Iraq. The authors also intend to use the precise differences in physical volcanology; morphometry; petrography and geochemistry to constrain the rates of magma extrusion, cooling histories and investigate their emplacement mechanism as well as to determine their origin and type of parental magma. The authors describe the lithostratigraphy, petrology and geochemistry for the two sections and discuss a possible scenario that explains the observed geochemical and morphological as well as lithostratigraphic variations in the area (Fig.2). The gained information from the present study of GPB is combined with the associated sedimentary rocks to

indicate the environment of deposition and geologic setting of the investigated area within Zagros Suture Zone and to investigate their relationship to the tectonic evolution of the whole region.

## 2. Geological Setting

Gole Pillow Basalt (The GPB) located along 35°46'34"N and 45°49'11.5"E with the altitude of 1176m above sea level, and about 21 Km NW of Penjween town and 43 Km NE of Sulaimani Governorate Kurdistan Region, NE Iraq (Fig. 1). Tectonically the investigated area located within Penjween- Walash zone in the Zagros Suture Zone.

[6], described Penjwin-Walash subzone, as a unit of the main (Central) Neo-Tethys, which comprises volcano-sedimentary sequences formed during Cretaceous ocean spreading in the Neo-Tethys, and Paleogene arc volcanics and syn-tectonic basic intrusions formed during the final closure of this ocean. The most remarkable unit of this subzone is the Qulqula group and well exposed in the area. Thereafter Bolton's work in 1958, many authors had been worked on Qulqula group like [13]; [14]; [6]; [8] and [10], and several attempts were made to divide Qulqula group into further smaller units.

The studied volcanic rocks are associated with the Qulqula Radiolarite and occur as massive continuous blocky outcrops. Most of the pillows well preserved but some pillows occasionally appeared and dissected making identification and measurements of pillow dimensions impossible (Fig. 1).

Lithostratigraphy and surrounding rocks of GPB are complex and still controversial (Fig. 2), as several authors mentioned and mapped Red Bed Series in the area, however, the authors in this study had never seen in the field. Despite the previous lithology a chocolate limestone beds contacted with the GPB have been found. Although, [5] described these limestone beds in Gole village as chocolate brown recrystallized limestone and like those seen in Walsh group, the authors believed that the limestone bed is return to Govanda Limestone Formation [15].

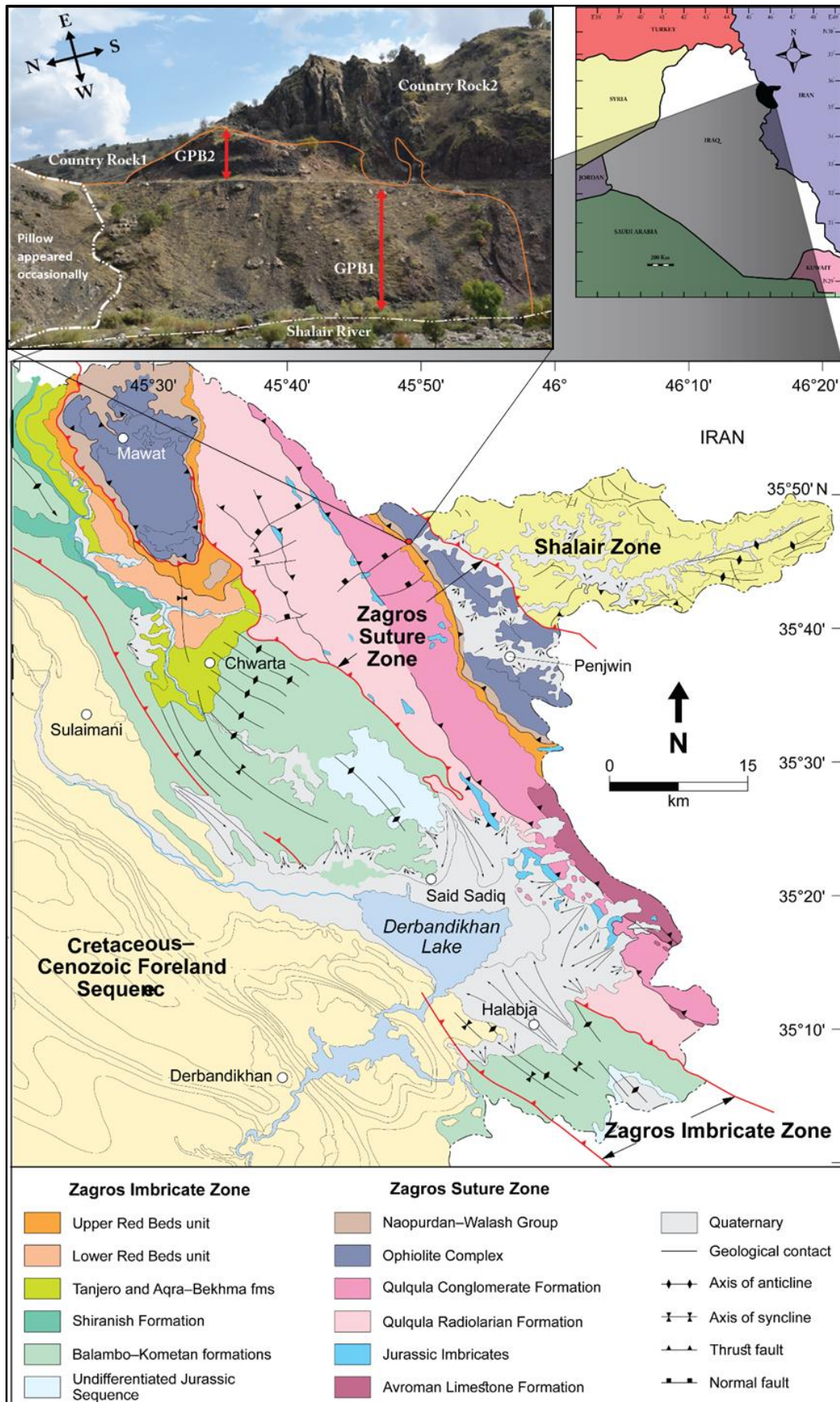


Fig. 1: Geologic map of the studied area after [8].

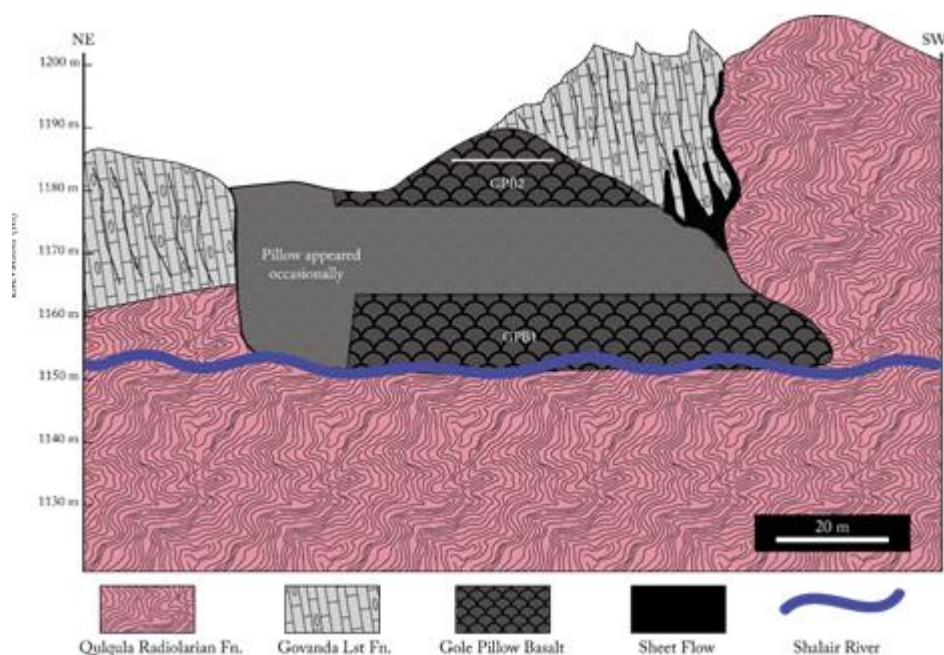


Fig. 2: The lithostratigraphy of GPB and surrounding rocks.

### 3. Sampling and Analytical Methods

Forty-five representative samples were systematically selected throughout the GPB rocks based on the pillow (Core, middle of pillow and rind) morphology and structures. Petrographic thin sections were prepared for all samples from both sections GPB1 and GPB2. The thin sections of these rocks were carefully studied using conventional refracted light microscopy. As well as for some of the minerals, the semiquantitative volume estimates were determined by visually estimating the mineral proportions in studied thin sections. About 200-300 g of clean, unaltered interior chips were selected from approximately 1-3 kilograms of sample material. The selected samples were crushed into centimetric dimensions and left for 5 days within HCl (Fig. 3), to remove pore minerals (Calcite) and avoiding errors in geochemical readings, especially for CaO%. Despite their similarity in composition, 12 samples (Relatively less altered less vesicular) for major elements and selected trace elements (Table 1) were analyzed using Axios-advanced X-ray fluorescence spectrometer at the Department of Geology at Sulaimani University, Iraq and school of earth science at Glasgow University, Scotland and University of Gothenburg, Sweden. The calibration was done against both international and internal Omnian standards of appropriate compositions. Geochemical data in Table 1 also contains standardized CIPW norms, Mg Numbers ( $Mg\# = \text{molar Mg} / (\text{Molar Mg} + \text{Molar Fe}) * 100$ ), and some rations calculations as well as Rock-types for all samples. All these calculations were automatically computed using both GCDKit [16] and Petrograph 2 beta [17] Computer Program.



Fig. 3: Shows samples preparation (left in HCl) for Geochemical analysis.

### 4. Morphology and Field Observations

The morphologic diversity of lavas erupted in the Gole area is significant, ranging in dimensions from centimetric to metric scale. Based on [18] classification scheme for pillow lava dimensions, the Gole pillow lavas can be classified both as normal-pillows (<100 cm in length) and mega-pillows (>1 to 3 meters in length) (Figs. 4 & 5B). One of the distinguishing aspects of the GPB having pillows well preserved and of different sizes, shapes and features among the two sections. Pillows in Gole area mostly appeared to be flattened and tubular with bread crust crack surfaces (Fig. 5C). Some pillows exhibit well preserved radial joints, which radiate from the central massive core of the pillow to the outer margins. Radial joints are spaced 10–20 cm apart. Each pillow is characterized by a massive core and chilled margin with a thickness from 3 to 8 cm (Fig. 5F).

Nature and morphological features of GPB vesicle appeared to be either small circular, incipient pipe vesicles and long fibrous in form. Distribution nature of these different forms of vesicles is a counterpart

with the fluid path within GPB. However, small circular vesicles distributed along the periphery of the pillow while the longer prism form of vesicles distributed from the center to the periphery of the pillow (Fig. 5D).

Although most of the vesicles were filled with secondary minerals some vesicles are unfilled (Fig. 5E). This is indicating two different environments.

For instance, those vesicles were filled with secondary minerals had an environment rich with secondary mineral ions and components. The latter one holds two ideas for interpretation. First, the pillows extruded within a very shallow water environment which lack dissolved ions. The second idea state that by erosional factor secondary minerals were removed away.



Fig. 4: Field photo pf the GPB, shows the distribution of the pillows within section2.

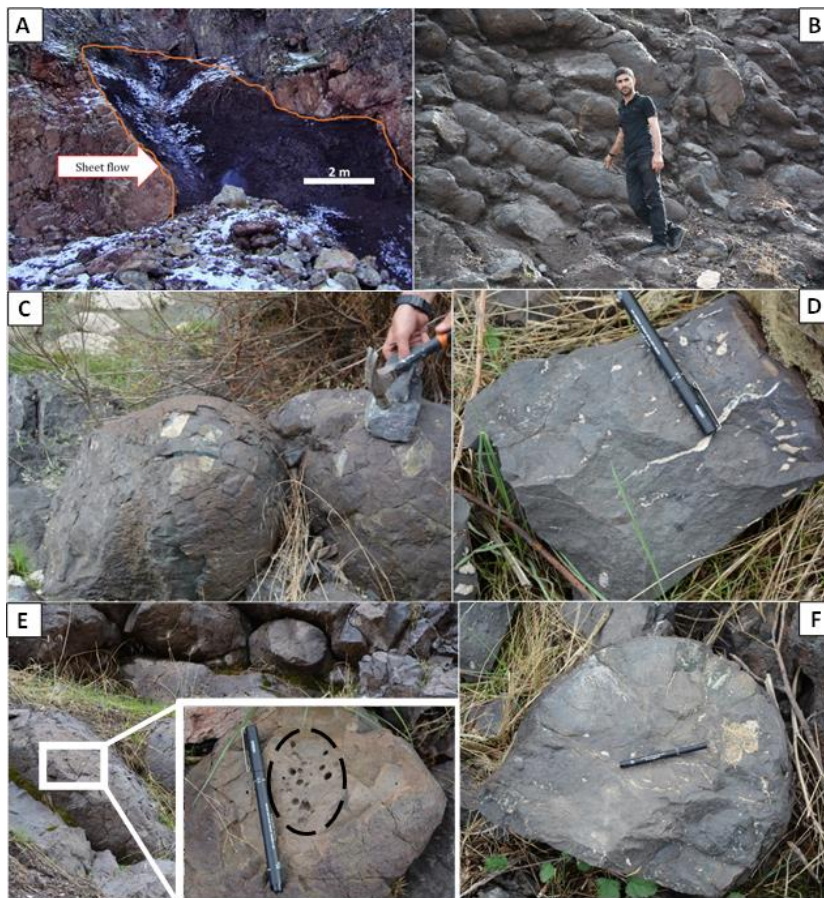


Fig. 5: Morphology and field observations of GPB, (a) Sheet flows of GPB, (b) normal and mega pillow forms almost 2.3 m sizes, (c) flattened and tubular pillow with bread crust crack surfaces, (d) Filled circular vesicles and longer prism, (e) unfilled vesicles and (f) Radial joints within pillows spaced about 10-20 cm and filled with secondary minerals.

## 5. Petrography

In the Gole area, the mafic volcanic rocks display aphyric texture and consist of the pillow with amygdaloidal and vesicular basalts. After careful and detail field works of GPB, more than 30 rock samples were collected for petrographic study. 10 of them specially selected for the petrographic study of amygdule constituents and the 20 others were chosen for detail petrographic study of essential and accessory mineral constituents.

Normative% of both essential and accessory constituents are variable according to the GPB sections (GPB section1 and 2) (Table 1). In the GPB Section1, the primary minerals are Albite (19–30%), Anorthite (22–28%), Hypersthene (7–17%), Hematite (15–17%) and Sphene (7–8%). The accessories are Quartz, Orthoclase, Diopside, Ilmenite, Chromite, Apatite and Zircon. While in the GPB Section2 the primary minerals represented by: Orthoclase (5–12%), Albite (15–23%), Anorthite (19–24%), Diopside (9–25%), Hypersthene (8–14%), Hematite (16–18%) and Sphene (7–8%). The accessories are Quartz, Ilmenite, Chromite, Apatite and Zircon. In addition, the

secondary minerals of the amygdules (in both sections) are represented by Calcite and Quartz.

Generally, in the thin sections there exist variations in mineral constituents, grain size and texture across the pillow core to rind contact. The pillow core shows predominantly sub-ophitic to the porphyritic texture while the rinds show palagonitized intersertal texture (Fig. 6a). Plagioclase (about 60% by volume) in the core occasionally occurs as microphenocrysts range in size less than (0.5 mm). The majority shows lath like, quenched and almost swallow-tailed in form and most of them appear with the dusty surface (Figures 6b and 6c). While Pyroxene dispersed within ferric groundmass has no clear form and represented by Hypersthene which shows a typical schiller structure (Fig. 6c). Other contents mostly are Fe-Ti oxide minerals including Hematite, Sphene and Ilmenite.

In terms of textures, GPB samples show different textures including vitrophyric texture which composed of sheaf-like radial clusters of plagioclases with scattered microphenocrysts of pyroxene in the interstices and opaque minerals dispersed in a glassy matrix (Fig. 6d).

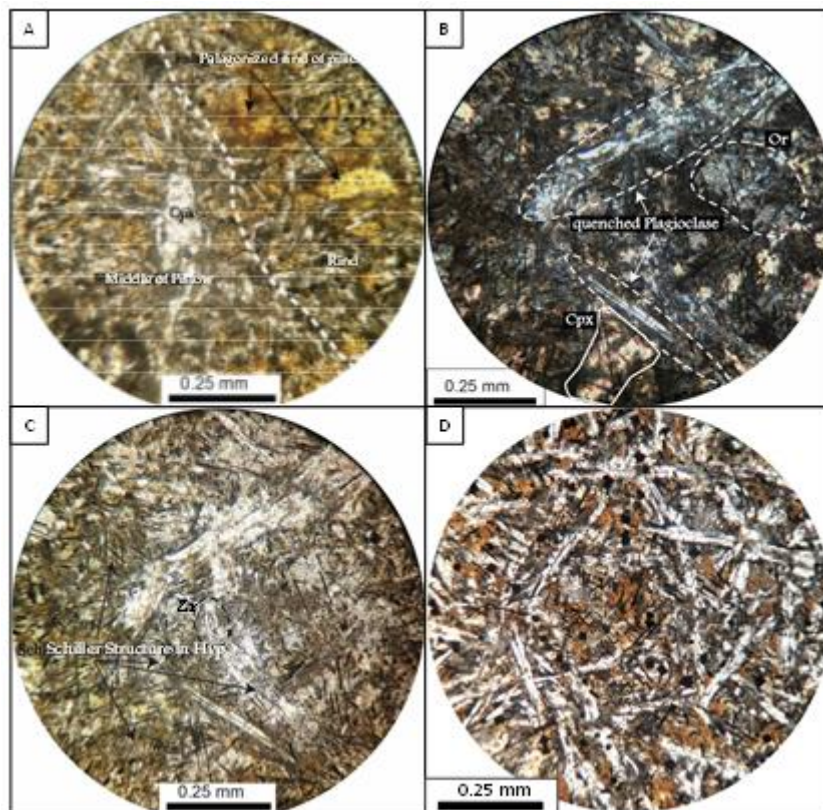


**Fig. 6:** (a) Showing the contact between middle and palagonitized rind of the pillow. (b) Showing quenched plagioclase grains. (c) Hypersthene schiller structure and Zircon grain. (d) Showing the glass with dispersed opaque minerals and medium-grained intersertal to intergranular and vitrophyric texture by Plagioclase grains within GPB thin sections.

## 6. Geochemistry

For geochemical classification and interpretation of the rock types, 12 samples were analyzed. The GPB samples were classified into two sections, section one

comprises GPB1-GPB7 samples and section two comprises GPB8-GPB12 samples (Table 1).

In the present study, the authors tend to describe the geochemistry of GPB in details. Therefore, a great number of geochemical diagrams presented in this

section to declare their geochemical characteristics and petrogenetic origin. Consequently, geochemical diagrams used based on a major; trace and major with trace elements, to cover best geochemical study as its first study for these rocks in the area.

GPB samples were plotted on the total alkali-silica (TAS) classification of either [19]; [20], and the PBG samples belong to basalts and Basalts to Tephrite-Basanite respectively (Figs. 7a & 7b). Although some samples especially PBS2 samples tend to be Tephrite to Basanite, all samples mentioned being of Alkaline Basalt using compositional field diagrams of  $P_2O_5\%$  vs  $TiO_2\%$  after [21] (Fig. 8), as well as the authors, believe that the PBS2 samples were possibly affected by weathering.

### 6.1 Major Elements

Major element compositions of GPB samples are shown in (Table 1). Generally, all samples of the two sections (GPB-section1 and GPB-section2) show the lowest variation in compositions. For the two sections,  $SiO_2$  concentration is ranging between (43.59-46.84) wt.% and (41.8-44.44) wt.% respectively.  $Al_2O_3$ ,  $TiO_2$  and  $MgO$  concentrations vary from (13.97-14.92) wt.%, (3.65-3.84) wt.% and (6.16-7.16) wt.% for GPB-section1 respectively. While in GPB-section2 they vary from (12.55-14.45) wt.%, (3.42-3.63) wt.% and (5.24-6.19) wt.% respectively. In the present study for all samples of the GPB the  $Fe_2O_3$  is calculated as total iron and show slight variation for both sections and vary from (14.84-17.27) wt.% and (15.99-19.23) wt.% respectively. The alkaline content, both  $Na_2O$  and  $K_2O$ , are high along with all GPB samples. The  $Na_2O$  content in the GPB-section1 vary from (2.25-3.55) wt.% and are higher than  $K_2O$  which vary from (0.19-1.07) wt.%, while in the GPB-section2 they show nearly equal content,  $Na_2O$  range between (1.96-2.71) wt.% and  $K_2O$  range between (0.9-2.54) wt.%.

The other contents also show lowest variations and will not exceed by 1 wt.%, except  $CaO$  content which shows slight variation between (6.83-10.48) wt.% for section one and (7.47-13.61) wt.% for section two.

The low content of  $MgO$  in all samples (Both sections) is related to the absence of Olivine and Amphibole (Mg-hornblende), while the higher content of  $Fe_2O_3$  represented by the high modal percent of Hematite and Hypersthene (Ferrosilite). As well as the  $TiO_2$  represent higher content and may relate to the modal presence of Titanite (Sphene) and Ilmenite.

Furthermore, using Harker diagrams most of the major oxides display a clear negative or positive correlation with increasing  $MgO$  content. These correlations are reflecting the major role of fractional

crystallization processes during the evolution of the GPB rocks. The trends for  $SiO_2$ ,  $CaO$ ,  $Na_2O$ ,  $TiO_2$  and  $Fe_2O_3$  versus  $MgO$  are suggestive of fractionation of Hypersthene, plagioclase, Sphene and other Fe-Ti oxides (Fig. 9).

### 6.2 Trace Elements

Trace element concentrations of GPB samples are shown in (Table 1). Generally, all trace elements of GPB samples are characterized by higher or close concentrations of fresh basalt. compatible trace elements concentrations like Cr, Co and Ni within GPB samples range between (70.5-157.6 ppm), (189.5-593.1 ppm) and (63.7-113.7 ppm) respectively. While Cr and Ni concentrations within fresh basalt range between (280-550 ppm) and (75-140 ppm) respectively after [22]. This decline in Cr concentration suggests spinel or clinopyroxene fractionation [23]. GPB samples also characterized by very high concentrations of both Cu and Zn and ranging between (439.7-1320 ppm) and (225.5-897.8 ppm) respectively, peculiarly if Cu concentration compared to fresh basalt, which in latter the Cu concentration ranges between (48-155 ppm). The higher concentration of Cu may reflect increasing fractional crystallization process [24]. While the authors believe that the high concentration of Cu is due to the presence of malachite and azurite ores around the GPB body.

The large ion lithophile elements (LILEs) among GPB are comprised (Rb, Sr and Ba) and their concentrations range between (19.2-78.2 ppm), (399.2-694.5 ppm) and (201.2-396.3 ppm) respectively. Despite the mentioned higher Sr concentration in GPB samples, Strontium concentration within fresh basalt range between (90-210) ppm [25] and state that Sr concentration seems to be decreasing with increasing alteration processes. The other trace elements are high field strength elements (HFSEs) within GPB and represented by (Zr, Nb and Y) their concentrations range between (334.8-410 ppm), (53.7-67.4 ppm) and (32.2-56.5 ppm) respectively.

For the study of chemical variation of the GPB, selected trace elements (Nb, Ba, Zr, Y, Rb, Sr, Ce and Zn) were correlated with  $MgO$ . Positive and negative correlations in the plots of the contents of some incompatible trace elements vs.  $MgO$  (wt. %) are observed in the GPB (Fig. 10). Both Nb and Zr show positive correlations with increasing  $MgO$  and they show the same linear correlations of the global Zr-Nb of OIB [26]. While Ba, Rb and Ce show negative correlations, the other trace elements show no obvious trends.

**Table 1: Major oxides (wt.%) and trace element (ppm) composition of Gole Pillow Basalt. AB: represent alkaline Basalt rock type.**

	Section 1							Section 2				
	GPB1	GPB2	GPB3	GPB4	GPB5	GPB6	GPB7	GPB8	GPB9	GPB10	GPB11	GPB12
<b>Major Oxides%</b>												
SiO <sub>2</sub>	45.32	46.43	45.24	45.11	45.10	43.59	46.84	44.26	44.41	41.80	44.44	43.88
Al <sub>2</sub> O <sub>3</sub>	14.06	14.48	14.01	14.24	14.44	13.97	14.92	13.60	13.70	12.55	13.68	14.45
TiO <sub>2</sub>	3.71	3.73	3.74	3.65	3.84	3.69	3.80	3.53	3.56	3.42	3.63	3.60
MgO	6.90	6.74	6.95	7.16	6.90	6.62	6.16	5.94	5.61	5.24	5.26	6.19
Fe <sub>2</sub> O <sub>3</sub>	16.55	17.27	16.88	17.19	16.66	16.42	14.84	19.23	18.58	17.95	17.32	15.99
CaO	8.10	6.83	8.18	7.27	8.54	10.48	8.74	7.47	8.01	13.61	10.15	10.81
Na <sub>2</sub> O	3.55	3.00	3.13	3.21	3.10	2.72	2.25	2.38	2.30	2.06	1.96	2.71
K <sub>2</sub> O	0.19	0.46	0.19	0.73	0.46	1.07	1.02	2.21	2.54	2.08	2.22	0.90
MnO	0.20	0.20	0.19	0.21	0.19	0.27	0.29	0.23	0.23	0.19	0.18	0.16
P <sub>2</sub> O <sub>5</sub>	0.66	0.54	0.69	0.54	0.65	0.72	0.70	0.72	0.72	0.77	0.76	0.73
<b>Total</b>	<b>99.23</b>	<b>99.68</b>	<b>99.21</b>	<b>99.30</b>	<b>99.89</b>	<b>99.54</b>	<b>99.56</b>	<b>99.57</b>	<b>99.64</b>	<b>99.67</b>	<b>99.61</b>	<b>99.41</b>
Mg#	45.23	43.60	44.92	45.21	45.07	44.40	45.13	37.96	37.43	36.64	37.56	43.40
ClA%	40.38	44.80	40.92	42.48	40.61	36.14	41.90	40.60	39.39	29.23	36.22	36.55
<b>Trace elements</b>												
Cr	157.6	107.5	77.7	118.1	134.3	109.8	77.1	101.4	70.5	101.2	94.6	121.5
Co	230.3	236.9	201.6	593.1	219.4	194.7	189.5	213.0	239.7	185.0	238.9	194.6
Ni	113.7	106.2	106.3	89.5	135.7	91.0	94.4	75.5	63.7	97.6	85.8	105.9
Cu	881.5	635.9	912.5	113.0	1320.0	1015.0	1030.0	774.4	700.5	586.3	590.7	439.7
Zn	560.8	314.0	527.9	549.0	897.8	621.6	225.5	496.1	471.0	363.1	429.2	253.8
Rb	23.0	19.2	20.0	21.0	22.0	24.6	21.0	62.9	77.8	78.2	64.6	20.3
Sr	399.2	435.3	400.5	541.0	526.0	558.8	694.5	548.9	500.6	487.4	576.7	646.8
Y	48.3	35.3	53.4	47.9	56.5	53.9	50.2	35.8	32.2	47.4	43.4	45.1
Zr	391.4	385.6	399.0	410.0	403.5	359.3	396.5	363.2	367.3	334.8	379.6	395.4
Nb	58.8	57.0	67.2	66.5	61.5	56.1	67.4	62.1	55.8	53.7	56.5	54.9
Ba	289.0	208.0	285.0	201.2	292.0	392.2	323.5	301.8	389.9	240.1	396.3	287.1
Ce	179.1	175.0	162.5	165.0	146.8	189.2	177.3	227.8	180.0	190.0	183.0	173.7
W	142.1	122.2	154.9	755.9	169.6	131.4	217.7	73.3	151.0	160.0	200.9	144.3
<b>CIPW norm</b>												
Quartz	1.14	5.25	3	1.06	1.51	0	6.24	1.74	1.1	0	2.06	0
Orthoclase	1.14	2.7	1.13	4.34	2.71	6.32	6.03	13.05	14.99	12.29	13.13	5.31
Albite	30	25.36	26.45	27.14	26.23	23.01	19.03	20.15	19.45	15.69	16.59	22.92
Anorthite	21.9	24.72	23.63	22.29	24.13	22.76	27.61	19.89	19.57	18.87	21.96	24.61
Diopside	1.6	0	0.31	0	1.23	10.13	0	1.04	3.28	25.44	9.17	9.84
Hypersthene	16.5	16.77	17.17	17.83	16.62	7.13	15.34	14.31	12.44	0	8.85	9.2
Olivine	0	0	0	0	0	3.26	0	0	0	0.88	0	1.16
Hematite	16.6	17.27	16.88	17.19	16.66	16.42	14.84	19.23	18.58	17.95	17.32	15.99
Sphene	8.54	4.12	8.62	7.37	8.87	8.31	8.09	8.03	8.09	7.85	8.4	8.37
Ilmenite	0.43	0.44	0.43	0.46	0.43	0.58	0.62	0.49	0.49	0.42	0.4	0.36
Apatite	1.56	1.28	1.63	1.28	1.55	1.7	1.65	1.7	1.7	1.83	1.8	1.73
Chromite	0.03	0.02	0.02	0.03	0.03	0.02	0.02	0.02	0.02	0.02	0.02	0.03
Zircon	0.08	0.08	0.08	0.08	0.08	0.07	0.08	0.07	0.07	0.07	0.08	0.08
Cr/Ni	1.39	1.01	0.73	1.32	0.99	1.21	0.82	1.34	1.11	1.04	1.10	1.15
Rb/Sr	0.06	0.04	0.05	0.04	0.04	0.04	0.03	0.11	0.16	0.16	0.11	0.03
Zr/Nb	6.65	6.76	5.94	6.17	6.56	6.40	5.88	5.85	6.58	6.24	6.72	7.20
Zr/Y	8.11	10.92	7.47	8.56	7.14	6.67	7.90	10.15	11.39	7.06	8.75	8.77
Y/Nb	0.82	0.62	0.79	0.72	0.92	0.96	0.74	0.58	0.58	0.88	0.77	0.82
Nb/Y	1.22	1.61	1.26	1.39	1.09	1.04	1.34	1.73	1.73	1.13	1.30	1.22
Al <sub>2</sub> O <sub>3</sub> /TiO <sub>2</sub>	3.79	3.89	3.75	3.90	3.76	3.78	3.93	3.85	3.85	3.67	3.77	4.02
<b>Rock Name</b>	<b>AB</b>											

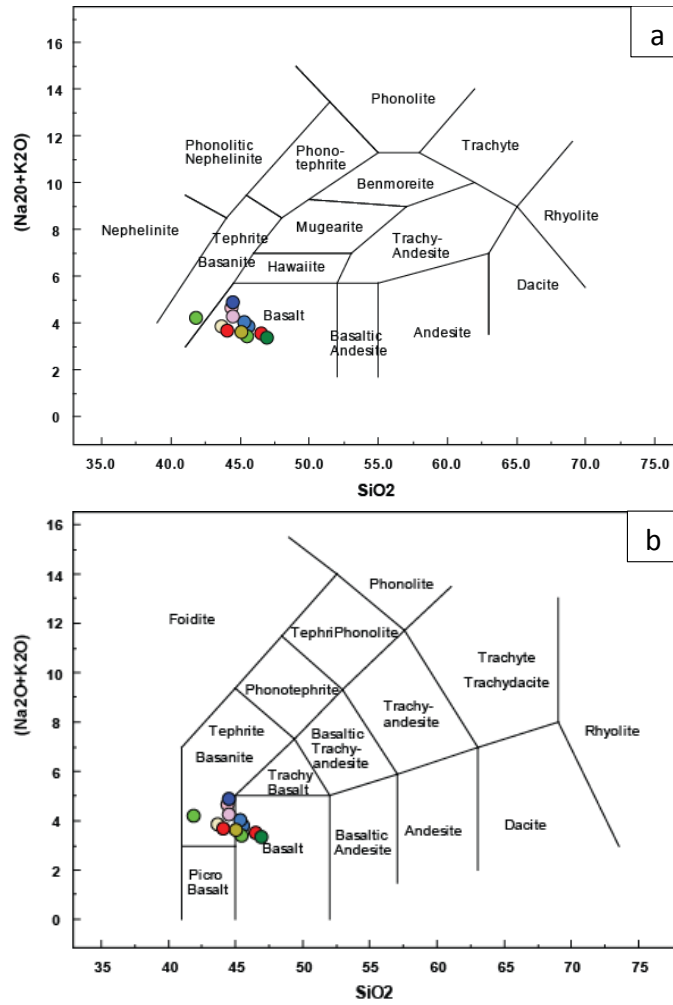


Fig. 7: TAS Alkalies-Silica Diagrams, (a) After [19], all GPB samples located on Basalts except 1 sample tends to be Tephrite Basanite. (b) after [20], most GPB samples located on Basalts and some samples tend to be Tephrite Basanite.

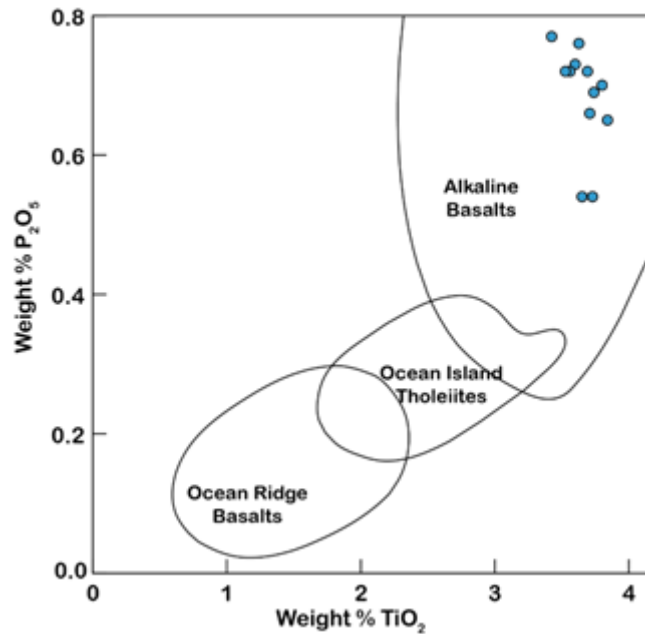


Fig. 8: GPB whole-rock geochemical data of TiO<sub>2</sub> Vs P<sub>2</sub>O<sub>5</sub> plot, compositional fields after [21].

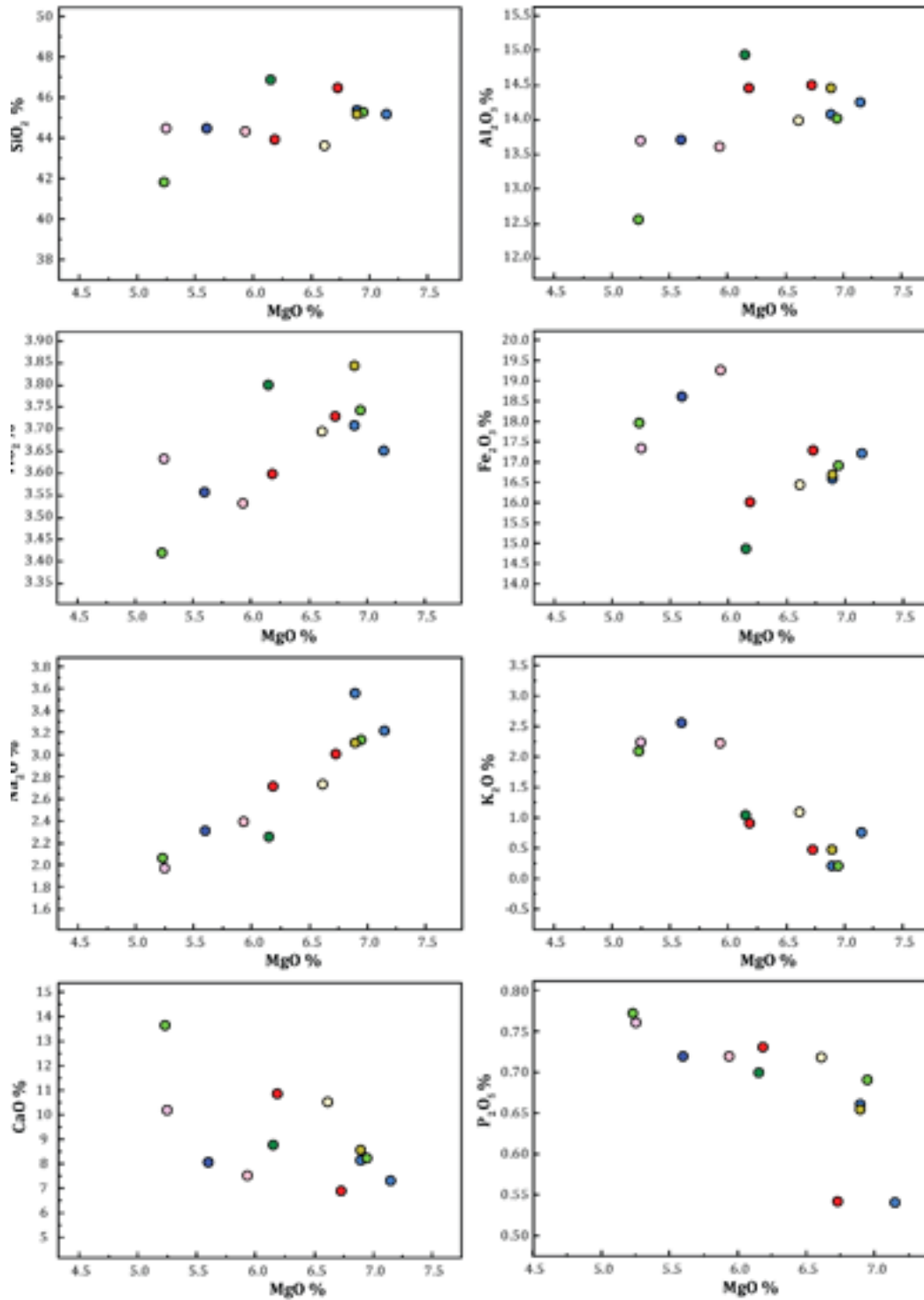


Fig. 9: Harker MgO variation diagrams for selected major elements in GPB rocks.

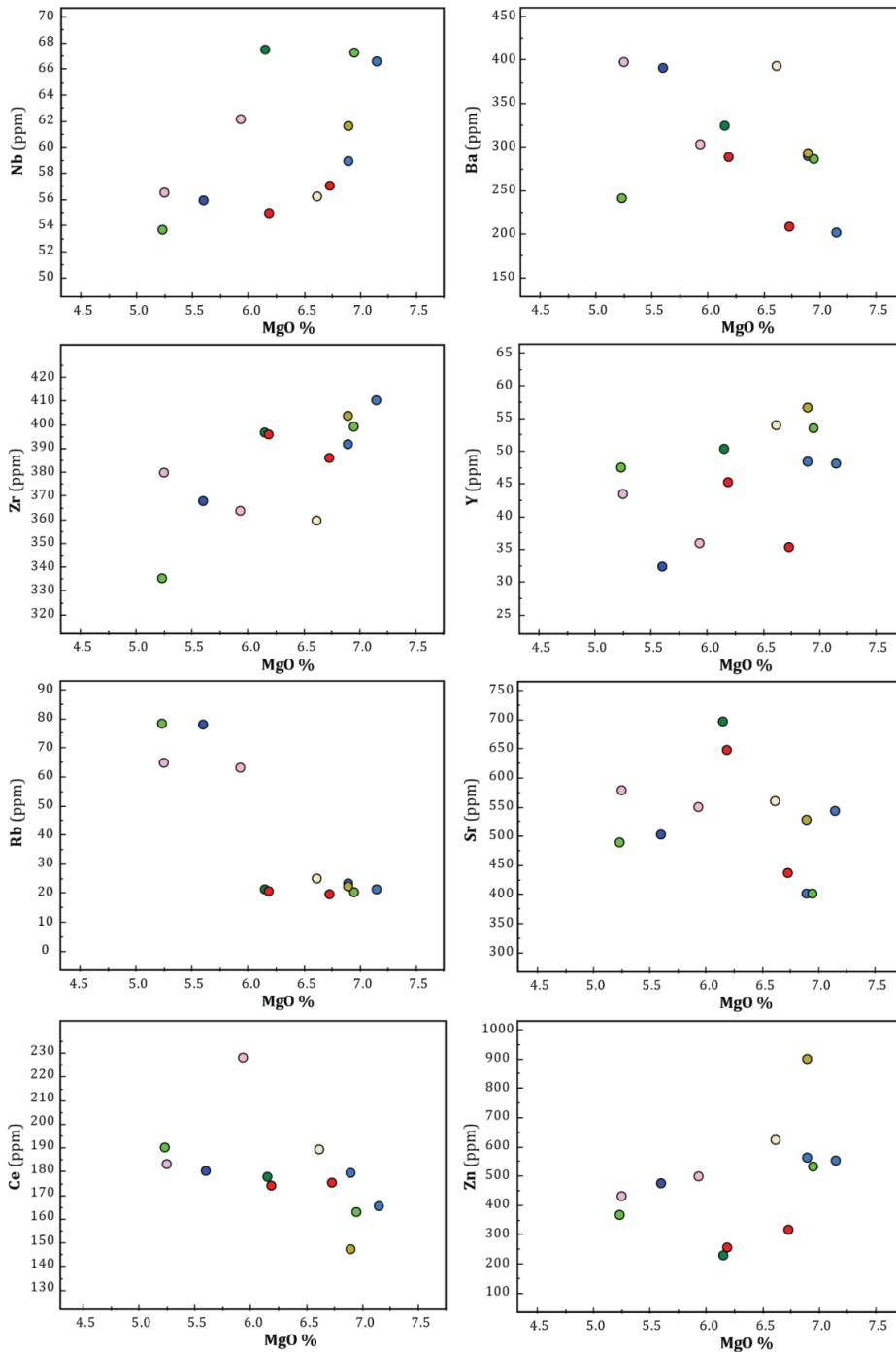


Fig. 10: Harker MgO variation diagrams for selected trace elements in GPB rocks.

**7. Discussion**

The volcanic rocks of the Penjween area in general and the GPB rocks, in particular, are among the least-studied parts of the Zagros Suture Zone basalts. Although several studies have dealt with the submarine basaltic rocks of the ZSZ (e.g. [5]; [6]; [7]; [8]; [9]; [10] and [11] and it's not the first attempt to find pillow basalts within Qulqula radiolarian group, but finding such fresh pillow basalts and in these morphologies is a unique investigation. Field investigation of the GPB yield that the studied pillows are fresh and well preserved. Moreover, to answer the question if the GPB samples influenced by

alteration, the authors used the CIA (Chemical Index of Alteration) value method. In this method, the major element contents can be measured by CIA value  $[Al_2O_3 / (Al_2O_3 + CaO + Na_2O + K_2O)] * 100$  in molecular proportions after [27]. The CIA values of the GPB samples range from (29.23%) to (44.8%) and most of them are in the range of 36%–40% (Table 1), consistent with the CIA values of fresh basalts (CIA=30–45%, [27]). It indicates no significant changes to the major elements of the GPB. Several geochemical characters have been used to indicate the alkaline robust nature of these rocks like Nb/Y ratios  $\geq 1.4$  (Fig. 11) and these basaltic rocks

have relatively high  $\text{TiO}_2$  (3.42–3.84 wt.%) and  $\text{P}_2\text{O}_5$  (0.54–0.77 wt.%) contents (Fig. 8), as well as display significant enrichment in Nb. These properties are highly similar to those observed in typical ocean island basalts (OIB) [28], suggesting that magmas of these rocks in the Gole area may have originated from an OIB-like mantle source.

Although [15] concluded that the studied area was an intercontinental shallow basin by studying stratigraphy of Govanda Formation, the authors also tend to use morphological features like (vesicles and pipe vesicles diameter size and distributions as well as pillow forms and sizes) and compared to the studies of [29];[30];[18];[4] and all indications point that the GPB extruded in a shallow marine environments with a depth of about less than 350m.

Below we consider the implications of the new data we have presented and our new results regarding GPBs to interpret the petrogenesis and tectonic settings in which the GPB rocks formed.

### 7.1 Tectonic settings, petrogenesis and mantle source

As known in studying the geochemistry of igneous rocks, the essential step is the tectonic evaluation of the studied area. And since, each tectonic environment is characterized by the particular geochemical signature (e.g. [31];[32], for this purpose many discrimination diagrams have used to infer both tectonic environments and petrogenesis of GPB. Since a long time, several discrimination diagrams have been used by authors like [33]; [34]; [35] to distinguish different tectonic environments for Basalt. While in the last decades [36] has presented the concept of the classification tree to delimit different tectonic environment of formation. These tectonic settings are Ocean Island Basalt (OIB), mid-ocean ridge Basalt (MORB), and island arc Basalt (IAB).

According to the classification tree of [36], all GPB samples resemble the OIB tectonic environment as their  $\text{TiO}_2$  % are greater than 2.13%. As well as using the Si–Ti–Sr linear discrimination diagram after [36], all GPB samples correspond OIB field again (Fig. 12). In addition, some chemical ratios of the GPB samples are also compared to those proposed by [37] and [38]. All GPB samples tend to resemble precisely OIB which indicating the presence of OIB rocks in Penjween area within ZSZ (Table 2).

Considering several tectonic discrimination diagrams like (Figs. 13 to 17), it is seen that the GPB samples in the present study are clearly prevailed by Within Plate Basalt (WPB). In the Zr/Y versus Zr tectonic discrimination diagram as defined by [39], the GPB samples indicate a within-plate environment (Fig. 13). As well as, using binary tectonic discrimination diagrams of Zr/Y vs Ti/Y after [40] and Ti vs Zr after [41], all GPB samples occupying the (WPB) field (Figs. 14 & 15 respectively). However, using Ti/Y vs Nb/Y discrimination diagrams of [41] GPB samples were fallen from transitional to alkaline WPB field (Fig. 16). Finally, on a more recent diagram of [42]

(using major elements of  $\text{TiO}_2$  vs  $\text{Al}_2\text{O}_3$ ), the GPB samples were plotted and occupied precisely the Within-Plate Basalt field (Fig. 17).

According to [43], GPB samples display an affinity to OIB-type basalts, indicating their derivation from the recycled component. Using the diagram of Zr/Y and Nb/Y ratios also confirm the involvement of a recycled component for the GPB alkaline samples and mode of emplacement of the magma is indeed a mantle plume (Fig. 18). In contrast to traditionally accepted, about basalt tectonic setting along Zagros suture zone, the authors believe that during ascending the magma has been recycled with the lithospheric mantle.

Using spider diagrams for selected trace elements, all GPB samples were normalized to Chondrites and compared with the same normalization for OIB after [28], indicating there is a typical coincide of OIB affinity (Fig. 19). in another spider diagram for normalized averages of all GPB samples with Chondrite and compared with Normalized OIB of [28], GPB samples precisely overlapped with the OIB affinity (Fig. 20). as well as, using un-normalized geochemical data of GPB samples and comparing with OIB, averages of GPB samples show the best overlap with the OIB affinity (Fig. 21).

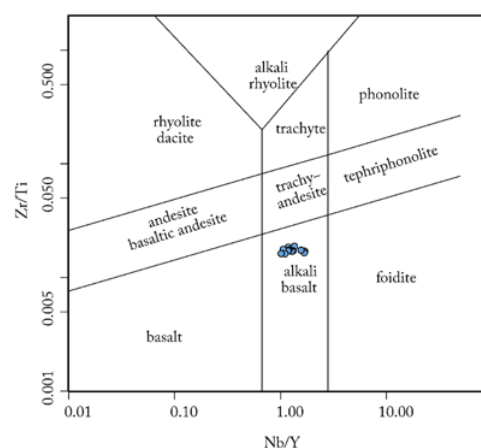


Fig. 11: Nb/Y- Zr/Ti plot modified by [44] indicating Alkaline nature of GPB rocks.

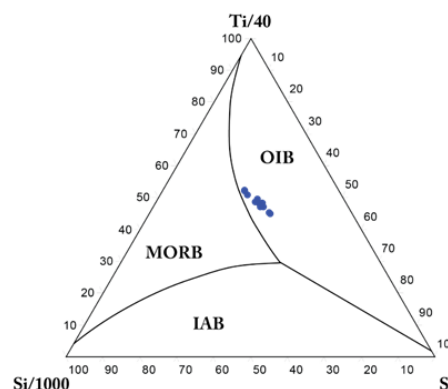


Fig. 12: The GPB data plotted on the Si–Ti–Sr linear discrimination diagram (Ternary) and resemble the OIB field, after [36].

Table (2): Comparison of some generalized geochemical ratios of pillow basalts from Gole Pillow Basalt (GPB) with some from N-MORB and OIB settings (N-MORB and OIB average ratios are from [38]).

	N-MORB	OIB	GPB
Zr/Nb	>30	<10	6.39
Ba/Nb	2,7	7,3	5.3
Ti/Zr	103	61	57.38
K/Rb	1067	368	196.08
P/Ce	69	34	16.6

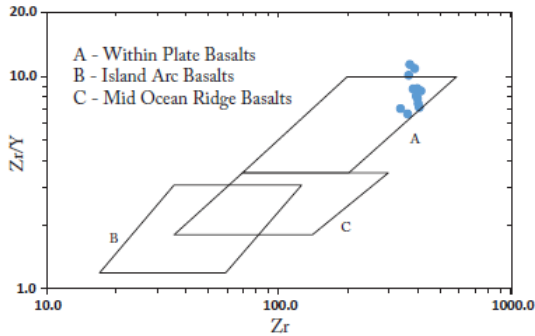


Fig. 13: Zr/Y vs Zr discrimination diagram for the GPB samples indicating within-plate alkali basalts, after [39].

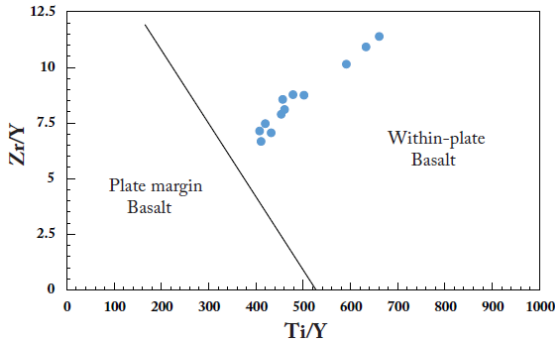


Fig. 14: The Zr/Y vs Ti/Y Discrimination diagram for GPB samples showing the fields of Within-plate Basalt and Plate Margin Basalt after [40].

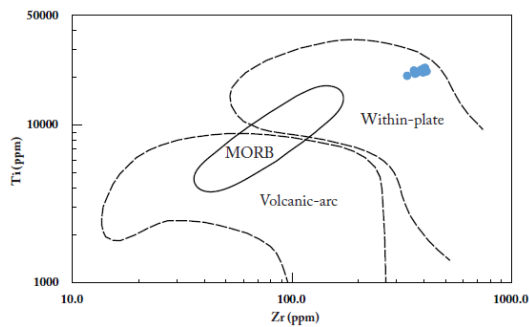


Fig. 15: Discrimination diagram for GPB samples based on Ti-Zr variations [41], all samples falling Within-plate Basalts.

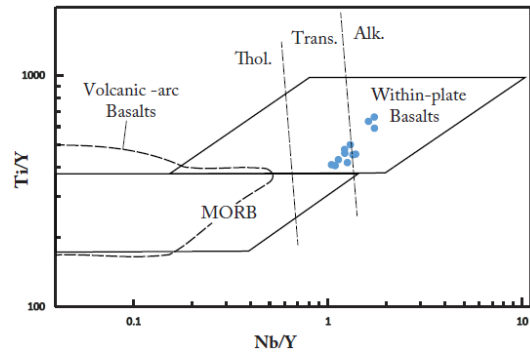


Fig. 16: The Ti/Y vs Nb/Y Discrimination diagram for GPB samples showing the fields of Within-plate Basalts, MORB and Volcanic-arc Basalts (dashed line). The Within-plate Basalts may be divided into tholeiitic (Thol.), Transitional (Trans.) and Alkali (Alk.) Basalt types [41].

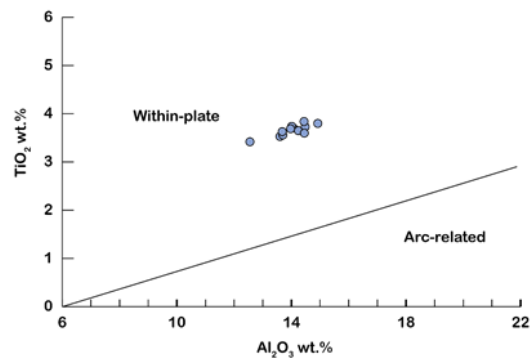


Fig. 17: The TiO<sub>2</sub> vs Al<sub>2</sub>O<sub>3</sub> discrimination diagram, all GPB samples precisely occupy the Within-Plate Basalt field, [42].

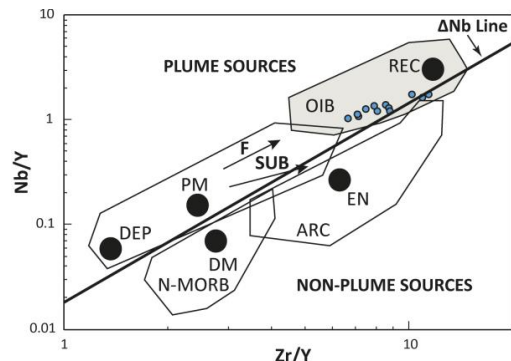
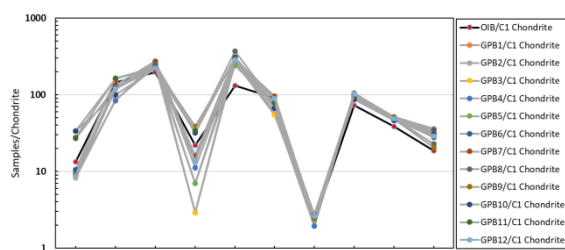
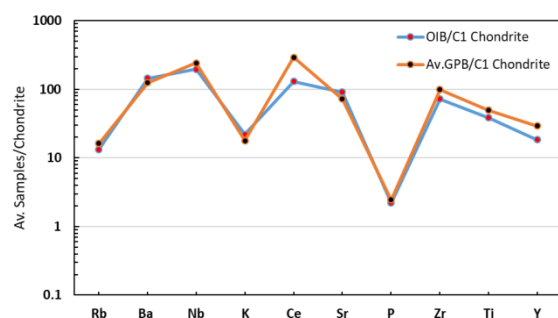


Fig. 18: Nb/Y vs Zr/Y diagrams illustrating probable mantle sources from which the studied samples derived [43]; arrows indicate effects of batch melting (F) and subduction (SUB), the straight line indicates  $\Delta Nb$ , fields are based on [45]; [46]. REC=Recycled Component; OIB=Oceanic Island Basalt; DEP=Deep Depleted Mantle; DM=Shallow Depleted Mantle; EN= Enriched Component.



**Fig. 19: Spider diagram for normalized GPB samples with Chondrite and compared with Normalized OIB of [28].**



**Fig. 20: Spider diagram for normalized averages of all GPB samples with Chondrite and compared with Normalized OIB of [28].**

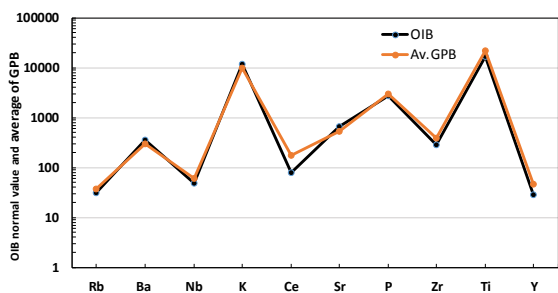


**Fig. 21: Spider diagram for selected trace elements for averages of all GPB samples and compared with OIB data of [28].**

## 8. Conclusion

The pillow basalts, associated with the Qulqula radiolarian group, are well exposed at two different localities in the Gole area. On the basis of the present

## References

- [1] Winter, J.D. (2001). An introduction to igneous and metamorphic petrology. 1<sup>st</sup> edn., Prentice-Hall Inc.: Upper Saddle River, New Jersey 07458: 697pp.
- [2] Umino, S.; Lipman, P. W. and Obata, S. (2000). Subaqueous lava flow lobes, observed on ROV KAIKO dives off Hawaii. *Geology*, **28** (6):503-506.
- [3] Moore, J. G. (1975). Mechanism of Formation of Pillow Lava. *American Scientist*, **63** (3):269-277.
- [4] Gregg, K. P. G. and Fink, J.H. (1995). Quantification of submarine lava-flow morphology through analogue experiments. *Geology*, **23** (1):73-76.
- [5] Buday, T. and Jassim, S.Z. (1987). The regional geology of Iraq: Tectonism, magmatism and metamorphism. 2<sup>nd</sup> edn., Baghdad: State Establishment of Geological Survey and Mineral Investigation: 352pp.

investigation on the selected unaltered site, it is concluded that –

- GPB consist of fresh well preserved and of different sizes ranging from normal to mega pillows.
- Field observations, morphology and stratigraphy of these rocks confirm that they are composed of sheet flow, pillow breccia and normal to mega pillows and they are extruded in a shallow marine environment with a depth less than 350m.
- Petrographically GPB samples are classified as aphyric and phyrlic types. Aphyric GPB samples show intersertal or variolitic textures, as well as phyrlic samples, exhibit porphyritic and sub-ophitic textures. Mineral constituents represented by quenched plagioclase, pyroxene, hematite and ilmenite as essential phases. While the accessories minerals are quartz, diopside, orthoclase, chromite, apatite and zircon.
- Using compositional field diagrams, based on major element geochemistry, classify the GPB samples as alkaline basalts.
- All investigated criteria for these rocks consist that GPB rocks were generated in within-plate oceanic island setting (OIB) and emplaced in a shallow marine marginal within plate basin.
- Trace element geochemistries confirm the involvement of a recycled component for the GPB alkaline samples and mode of emplacement of the magma is indeed a mantle plume.
- Further works on the mineral chemistry and geochronology of these basaltic will clarify the relationships and ages between the Qulqula radiolarian rocks and the studied Pillow lava as well as the time of the emplacement of these rocks.

## Acknowledgements

The authors gratefully acknowledge both the universities of Sulaimani in Kurdistan region-Iraq and the University of Gothenburg in Sweden for doing geochemical analysis for this project. The first author would like to thank Mr Awara, Earth Science Department, the University of Glasgow for his help in geochemical analysis.

- [6] Jassim, S.Z. and Goff, J.C. (2006). Geology of Iraq. 1<sup>st</sup> edn., Dolin: Prague and Moravian Museum, Brno, Czech Republic: 341pp.
- [7] Ibrahim, A.O. (2009). Tectonic style and evolution of the NW segment of the Zagros fold-thrust belt, Sulaimani Governorate, Kurdistan Region, NE Iraq. PhD thesis, University of Sulaimani, Iraq: 197 pp.
- [8] Al-Qayim, B.; Omer, A. and Koyi, H. (2012). Tectono stratigraphic overview of the Zagros Suture Zone, Kurdistan Region, Northeast Iraq. *Geo Arabia* **17** (4):109-156.
- [9] Ali, S.A.; Buckman, S.; Aswad, Kh.J.; Jones, B.G.; Ismail, S.A. and Nutman, A.P. (2013). The tectonic evolution of a Neo-Tethyan (Eocene–Oligocene) island-arc (Walash and Naopurdan

- groups) in the Kurdistan region of the Northeast Iraqi Zagros Suture Zone. *Island Arc*, **22** (1):104–125.
- [10] Baziany, M.M.Q. (2014). Depositional systems and sedimentary basin analysis of the Qulqula radiolarian formation of the Zagros suture zone, Sulaimani area, Iraq Kurdistan region. PhD Dissertation, Sulaimani University, Iraq: 178pp.
- [11] Zurar, S.S. (2016). Petrology and Isotope Dating of Volcanic Rocks within Qulqula Radiolarite, Iraqi Kurdistan Region. MSc Thesis, University of Sulaimani, Iraq: 147pp.
- [12] Saccani, E.; Dilek, Y.; Marroni, M. and Pandolfi, L. (2015). Continental margin ophiolites of Neotethys: Remnants of Ancient Ocean–Continent Transition Zone (OCTZ) lithosphere and their geochemistry, mantle sources and melt evolution patterns. *Episodes*, **38** (4):230-249.
- [13] Bolton, C.M.G. (1958). Geological map-Kurdistan series, scale 1/100,000 sheet K4, Rania. Geological Survey and Mining, Site Investigation: Baghdad: 1-36 pp.
- [14] Czech Team, (1976). Geological map of thrust belt, NE Iraq, (1:100,000). Iraqi Geological Survey and Mineral Investigation: Baghdad, Iraq.
- [15] Karim K.H. et al. (2018). Stratigraphy and Facies Analysis of the Govanda Formation from Western Zagros, Kurdistan Region, Northeastern Iraq. *Iraqi National Journal of Earth Sciences*, **18** (2):69-98.
- [16] Vojtech, J.; Colin M.F. and Vojtech, E. (2011). Geochemical Data Toolkit computer program for Windows written in R language, version 3.0 released to date (Sept. 2011). *Czech Geological Survey*.
- [17] Petrelli, M.; Poli, G.; Perugini, D. & Peccerillo, A. (2005). PetroGraph: A new software to visualize, model, and present geochemical data in igneous petrology. *Geochemistry Geophysics Geosystems*, **6** (7):1-15.
- [18] Walker, G.P.L. (1992). Morphometric study of pillow size spectrum among pillow lavas. *Bulletin of Volcanology*, **54** (6):459-474.
- [19] Cox, K.J.; Bell, J.D. and Pankhurst, R.J. (1979). *The Interpretation of Igneous Rocks*. 1<sup>st</sup> edn., Australia: George Allen and Unwin: 464 pp.
- [20] Le Bas, M.J.; Le Maitre, R.W.; Streckeisen, A. and Zanettin, B. (1986). A chemical classification of volcanic rocks based on the total alkali-silica diagram. *Journal of Petrology*, **27** (3):745-750.
- [21] Ridley, W.I. et al. (1974). Basalts from Leg 6 of the deep-sea drilling project. *Journal of Petrology*, **15** (1):140-159.
- [22] Humphris, S.E. and Thompson, G. (1978). Trace element mobility during hydrothermal alteration of oceanic basalts. *Geochimica et Cosmochimica Acta*, **42** (1):127-136.
- [23] Best, M.G. (2003). *Igneous and Metamorphic Petrology*. 2<sup>nd</sup> edn., USA: Blackwell Science Ltd.: 729 pp.
- [24] Krauskopf, K.B.(1979). *Introduction to Geochemistry*. 2<sup>nd</sup> edn., New York: McGraw-Hill: 617 pp.
- [25] Berndt, M.E.; Seyfried, W.E. and Beck, J.W. (1988). Hydrothermal alteration processes at mid oceanic ridge: experimental and theoretical constrains from Ca and Sr changes exchange reactions and Sr isotopic ratios. *Journal of Geophysical Research*. **93** (B5): 4573-4583.
- [26] Kamber, B.S. and Collerson, K.D. (2000). Zr/Nb systematics of ocean island basalts reassessed- the case for binary mixing. *Journal of petrology*, **41** (7):1007-1021.
- [27] Nesbitt, H.W. and Young, G.M. (1982). Early Proterozoic climates and plate motions inferred from major element chemistry of lutites. *Nature*, **299** (5885):269-277.
- [28] Sun, S.S. and McDonough, W.E. (1989). Chemical and isotopic systematics of oceanic basalt: implications for mantle composition and processes In: Saunders, A.d. and Norry, M.J. (eds.), *Magmatism on the oceanic basins. Geological Society of London*, **42** (1):313-345.
- [29] Moore, J.G. (1965). Petrology of Deep-Sea Basalt Near Hawaii. *American Journal of Science*, **263** (1):40-52.
- [30] Jones, J.G. (1969). Pillow Lavas as Depth Indicators. *American Journal of Science*, **267** (2):181-195.
- [31] Wood, D.A.; Joron, J.L. and Treuil, M. (1979). A reappraisal of the use of trace elements to classify and discriminate between magma series erupted in different settings. *Earth and Planetary Science Letters*, **45**:326-336.
- [32] Meschede, M. (1986). A method of discriminating between different types of mid-ocean ridge basalts and continental tholeiites with the Nb-Zr-Y diagram. *Chemical Geology*, **56** (3-4):207-218.
- [33] Pearce, J.A. and Cann, J.R. (1971). Ophiolite origin investigated by discriminant analysis using Ti, Zr and Y. *Earth Planetary Science Letters*, **12** (3):339-349.
- [34] Pearce, J.A. and Cann, J.R. (1973). Tectonic setting of basic volcanic rocks using trace element analyses. *Earth Planetary Science Letters*, **19** (2):290-300.
- [35] Rollinson, H.R. (1993). *Using Geochemical Data: Evaluation, Presentation, Interpretation*. 1<sup>st</sup> edn., Essex, UK: Longman Science and Technology: 344pp.
- [36] Vermeesch, P. (2006). Tectonic discrimination of basalts with classification trees. *Geochimica et Cosmochimica Acta*, **70** (7):1839–1848.
- [37] Winchester, J.A. and Floyd, P.A.(1977). Geochemical discrimination of different magma series and their differentiation products using immobile elements. *Chemical Geology*, **20**:325-343.
- [38] Floyd, P.A. (1991). *Oceanic Basalts*. 1<sup>st</sup> edn., Glasgow: Blackie and Son Ltd: Appendix D, 456-469.

- [39] Pearce, J.A. and Norry, M.J.(1979). Petrogenetic implications of Ti, Zr, Y and Nb variations in volcanic rocks. *Contributions to Mineralogy and Petrology*, **69** (1):33-47.
- [40] Pearce, J.A. and Gale, G.H. (1977). Identification of ore-deposition environment from trace element geochemistry of associated igneous host rocks. *Special Publication of the Geological Society of London*, **7**:14-24.
- [41] Pearce, J.A.(1982). Trace element characteristics of lavas from destructive plate boundaries. In: Thorpe, R.S.(Ed.), *Andesites: R.S. Wiley Interscience Incorporation, New York*: 525–548.
- [42] Muller, D.; Rock, N.M.S. and Groves, D.I. (1992). Geochemical discrimination between shoshonitic and potassic volcanic rocks in different tectonic settings: a pilot study. *Mineralogy and Petrology*, **46** (4):259-289.
- [43] Condie, K.C. (2005). High field strength element ratios in Archean basalts: a window to evolving sources of mantle plumes. *Lithos*, **79** (3-4):491–504.
- [44] Pearce J.A. (1996). A user's guide to basalt discrimination diagrams. In: Wyman D.A. (ed.) *Trace Element Geochemistry of Volcanic Rocks: Applications for Massive Sulphide Exploration. Short Course Notes 12. St. John's, Geological Association of Canada, Canada*: 79-113.
- [45] Weaver, B.L. (1991). The origin of ocean island basalt end-member compositions: trace element and isotopic constraints. *Earth and Planetary Science Letters*, **104** (2-4):381-397.
- [46] Condie, K.C. (2003). Incompatible element ratios in oceanic basalts and komatiites: tracking deep mantle sources and continental growth rates with time. *Geochemistry Geophysics Geosystems*, **4** (1):252-268.

## دراسة بترولوجية والجيوكيميائية لجولى وسادة بازلتيه في منطقة بينجوين، إقليم كردستان/شمال

### شرق العراق

جبار محمد أمين قرداغى ، يوسف عثمان محمد ، سالم امين عزيز

قسم علوم الارض ، كلية العلوم ، جامعة السليمانية ، السليمانية ، العراق

### الملخص

تم إجراء التحليلات البترولوجية والمورفومترية والجيوكيميائية للحمم الوسائدية من قرية جولى (مدينة بنجوين) بمدينة السليمانية شمال شرق العراق. قذف البازلت (GPB) Gole Pillow ، على شكل وسائد وجريان صفائحي إلى تكوين كلكلة الرايولاري (Qulqula radiolarite). يقتصر الاقتحام البازلتي على مساحة صغيرة تبلغ حوالي 100 متر مربع داخل منطقة بينجوين والاش في منطقة زاغروس التصادمي (ZSZ) في العراق. تم تقسيم المنطقة التي تمت دراستها إلى قسمين GPB1 و GPB2. اظهرت الدراسة ان هناك دفعتين من الانفجارات القلوية تحت سطح البحر التي أنتجت الحمم البركانية الوسائدية التي تفاعلت بشكل مختلف مع مياه البحر والتي نتج عنها صخور مختلفة من الناحية الشكلية والجيوكيميائية. وسادات القسم الاول (GPB1) مكشوفة بشكل جيد على طول نهر شلير بالقرب من قرية جولى. على الرغم من أن وسائد القسم الثاني (GPB2) قد تعرضت للتحلل بسبب التحول المنخفض الدرجة والعمليات الحرمائية المتأخرة ، إلا أن انسجتها النارية ما زالت محفوظة. عينات GPB هي في الغالب ناعمة (phyric) وتظهر بنسيج برفيري أو شبه اوفيتي.

من الناحية البترولوجية، ظهرت معظم عينات الصخور GPB بشكل صخور بازلت ناعم (aphanitic) وتظهر بشكل نسيج فقاعي ولوزي. توجد الحبيبات الكبيرة من معدن الهابيرستين مع تركيب شيلر داخل ارضية من حبيبات بلاجيوكليس طويلة. تنتشر في الأرض الأرضية العديد من الحبيبات الصغيرة كاملة الالوجه من المعادن المعتمة مثل الإلمنايت والهيماتايت.

الخصائص المورفولوجية لل GPB تظهر ان الوسائد المنفردة تظهر بشكل كروي وفصي الى شكل مستوي. على الرغم من أن بعض الوسائد تمتد على ارتفاع مترين بتوزيع شجري، ظهر البعض الآخر تظهر بشكل متصدع وباسطح ذات فواصل غير منتظمة وتكون الفقاعات مليئة جزئياً بالكالسايت والكوارتز .

من الناحية الجيوكيميائية، تبين ان هذه الصخور ذات محتوى عالي من  $TiO_2$  و  $Fe_2O_3$  و نسب عالية لكن من  $Zr/Nb$  و  $Zr/Y$ . استنادا الى محتوى القلوبات والنسبة العالية لل  $Nb/Y$  وحتوى السليكا وتوزيع العناصر الاثرية، فان هذه الصخور تصنف على انها صخور بازلت قلوية. المشاهدات الحقلية والعلاقات الطباقية و جيوكيميائية هذه الصخور المترافقة مع رواسب فتاتية و كاربوناتية تقترح ان الالافا الوسائدية قيد الدراسة قد تكونت في بيئة بحرية ضحلة وانها تكونت ضمن الجزر المحيطية ضمن الصفيح